Electronic Supplementary Material (ESI) for Green Chemistry.

Supporting Information

Identification of High Performance Solvents for the Sustainable Processing of Graphene

Horacio J. Salavagione[1], James Sherwood[2], Mario De bruyn[2], Vitaliy L. Budarin[2], Gary Ellis[1], James H. Clark[2*], Peter S. Shuttleworth[1*]

[1] Departamento de Física de Polímeros, Elastómeros y Aplicaciones Energéticas, Instituto de Ciencia y Tecnología de Polímeros, CSIC, c/ Juan de la Cierva, 3, 28006, Madrid (Spain).
[2] Green Chemistry Centre of Excellence, University of York, Heslington, York, Yorkshire, YO10 5DD (UK).

e-mail: peter@ictp.csic.es

Experimental

Materials. Graphite powder with a particle size of 45 μm was purchased from Aldrich (<45 micron, 99.99%, B.N. 496596-113.4G). CVD-graphene on Si covered with a SiO_2 layer of 90 nm was purchased from Graphenea, Spain. Triacetin and *N*-methyl-2-pyrrolidinone (NMP) were purchased from Sigma Aldrich. Dihydrolevoglucosenone (Cyrene) was obtained from Circa Group Pty Ltd, and later further purified by first passing the solvent through an alumina column and afterwards by vacuum distillation. The synthesis of Cyrene from cellulose *via* levoglucosenone has been previously reported (see Scheme 1).[1,2]

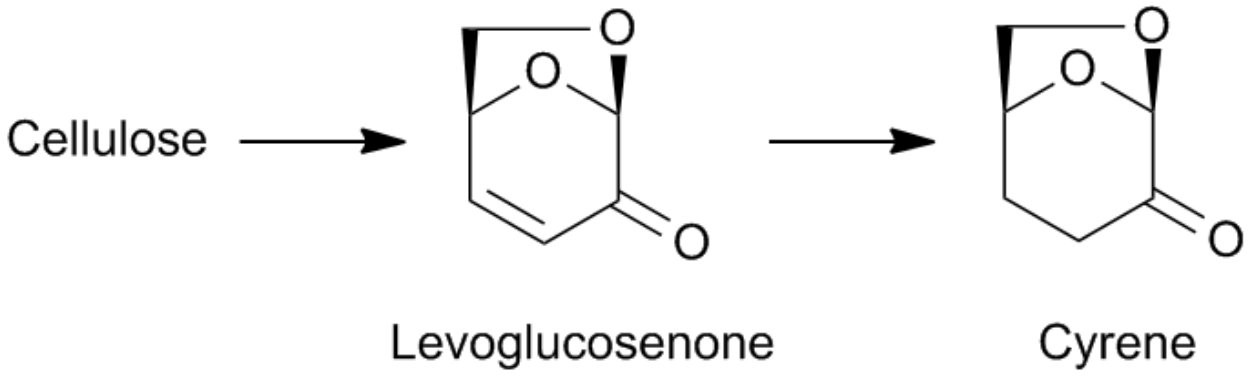

Scheme S1: Route of dihydrolevoglucosenone (Cyrene) production from cellulose via levoglucosenone.

All other materials were used as received.

Graphene solvent dispersion. The experimental procedure to disperse graphene was as follows: 3 mL of solvent was added to a vial containing ~ 4.5 mg of graphite (Aldrich, <45 micron, 99.99%, B.N. 496596-113.4G). The mixture was treated with an ultrasonic probe (UP400S ultrasonic processor, Hielscher) during 15 minutes and the resulting dispersions

were centrifuged at 7000 rpm for 10 minutes. The supernatant after centrifugation was transferred to a new vial by pipette.

Solvent dispersion concentration. UV-Vis absorption spectra of dispersed graphene in the solvents NMP, Cyrene, and triacetin were recorded on a Perkin Elmer Lambda 35 spectrophotometer and analysed using the dedicated Perkin Elmer UV Winlab v. 2.85.04 software, with the absorption spectrum shown in Figure S1.

For the UV calibration, 1 mL of centrifuged sample of graphene in Cyrene was passed through a fluoropore™ membrane (0.2 μm pore size) and the solid residue carefully weighed, accounting for any residual solvent to determine the actual dispersion of graphene. The same solution was diluted several times in order to prepare samples with different graphene concentrations. Using the UV absorbance at 660 nm,[3] where the spectra of the NMP and Cyrene dispersions both have a gradient of approximately zero, the observed magnitudes of absorbance were recorded. The variation of absorbance divided by cell length, as a function of the concentration of graphene dispersed in the reference solutions of Cyrene were plotted (see Figure 1c, main text) and the line of best fit used to calculate the molar absorptivity coefficient according to the Lambert-Beer law.

Contact angle. A computer controlled microscope Intel QX3 was used to measure the contact angle of the tested solvents. CVD-Graphene (on Si/SiO_2) pieces (Graphenea),[4] were placed on a manually controlled tilt table with a white light source to illuminate the sample from behind. With the microscope in the horizontal position, the shape of the static drops of the different solvents (3 μL) on the surface using a 60x objective were recorded at room temperature and pressure, and the contact angles calculated using a conventional drop shape analysis technique (Attension Theta optical tensiometer). Please also refer to Figure S3.

Solvent polarity. The calculation of Hansen solubility parameters and Hansen radii was performed with the HSPiP software package (4th Edition 4.1.04, developed by Abbott, Hansen and Yamamoto).

High resolution transmission electron microscopy (TEM). Both Cyrene and NMP dispersions were analysed using two types of TEM at the Centro Nacional de Microscopía Electrónica, Madrid, Spain with the aid of a technician, with TEM micrographs taken at random locations across the grids, to ensure a non-biased assessment. For measurement of graphene flake lateral dimensions, High-resolution HRTEM micrographs were performed on a JEOL JEM-2100 instrument (JEOL Ltd., Akishima, Tokyo, Japan), using a LaB6 filament, a lattice resolution of 0.25 nm and an acceleration voltage of 200 kV. For analysis of the graphene flake layers and molecular integrity of the graphene flakes, measurements were carried out on a High-resolution HRTEM micrographs were performed on a JEOL JEM-3000F instrument (JEOL Ltd., Akishima, Tokyo, Japan), using a LaB6 filament, a lattice resolution of 0.17 nm and an acceleration voltage of 300 kV. Directly after sonication and centrifugation the dispersion was added to an equal volume of acetone to dilute it as it was found that it was too concentrated to achieve a good TEM image, and secondly to aid evaporation of the solvent. Samples were prepared by drop-casting a few millilitres of dispersion onto holey carbon films (copper grids) and dried at 120 ºC under vacuum for 12 hours.

Raman spectroscopy characterisation. Raman measurements were undertaken in the Raman Microspectroscopy Laboratory of the Characterisation Service in the Institute of Polymer Science & Technology, CSIC using a Renishaw InVia-Reflex Raman system (Renishaw plc, Wotton-under-Edge, UK), which employed a grating spectrometer with a Peltier-cooled CCD detector coupled to a confocal microscope. The Raman scattering was excited with an argon ion laser (λ= 514.5 nm), focusing on the sample with a 100x

microscope objective (NA=0.85) with a laser power of approximately 2 mW at the sample. Spectra were recorded in the range between 1000 and 3200 cm^{-1}. All spectral data was processed with Renishaw WiRE 3.2 software. We would like to thank Ms. Isabel Muñoz Ochando from the Instituto de Ciencia y Tecnología de Polímeros de Madrid (ICTP), CSIC for help testing the samples.

Additional results

UV-vis dispersion analysis. The procedure for the preliminary analysis of the graphene dispersion with UV-vis spectroscopy is explained in the Methods section previously. The analysis permitting the calculation of graphene concentration is shown in Figure S1. The UV absorbance spectra are featureless above 500 nm (Cyrene starts to absorb below this value), but due to increased scattering caused by dispersed graphene particles in the case of Cyrene, its baseline is significantly higher than that of NMP and other solvents, indicative of a higher graphene concentration. Photographs of the dispersions immediately after centrifugation and one month later are shown in Figure S2.

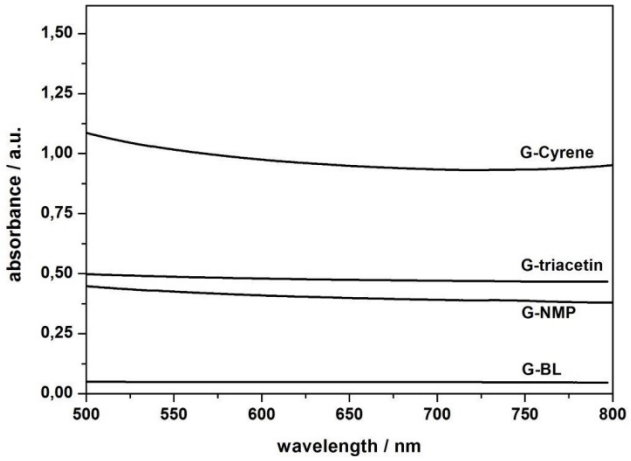

Figure S1. Spectroscopic analysis of graphene dispersion concentrations. The graph shows the UV-visible spectra of graphene dispersions in the solvents Cyrene (G-Cyrene), triacetin (G-triacetin), NMP (G-NMP), and butyl lactate (G-BL).

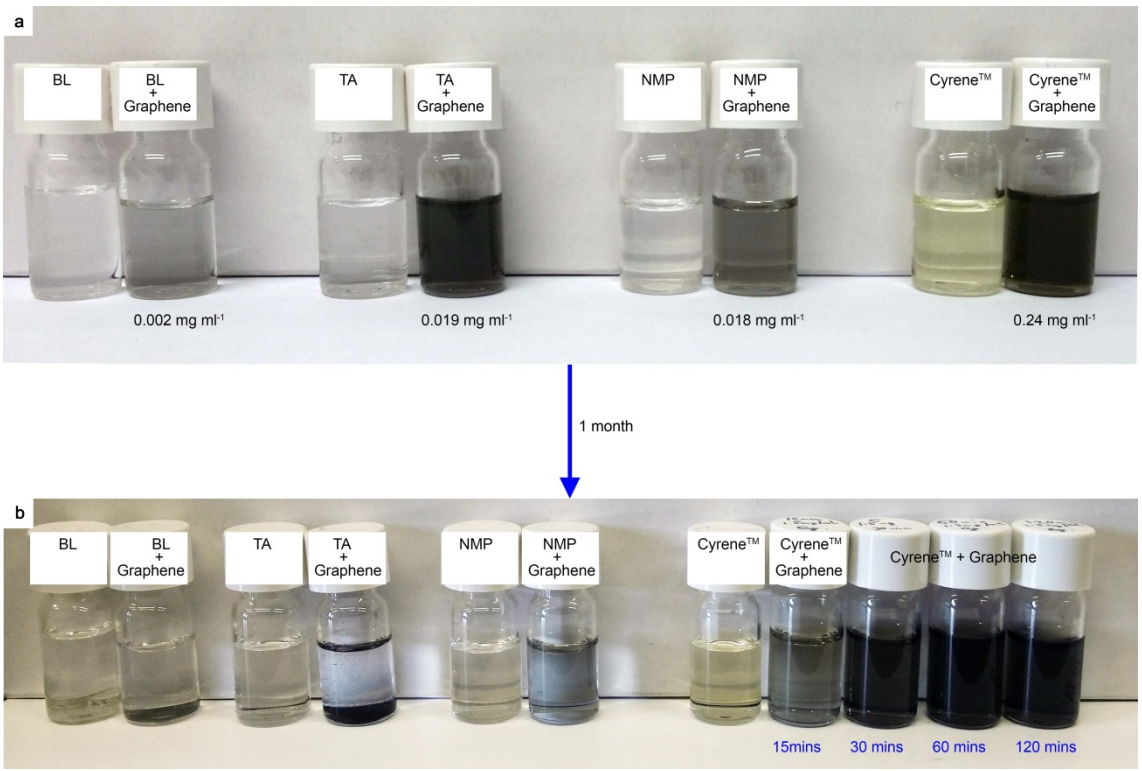

Figure S2. Pictures of the dispersed solvents after sonication and centrifugation. a) Graphene dispersions in butly lactate (BL), triacetin (TA), *N*-methyl-2-pyrrolidinone (NMP) and Cyrene compared to the original solvent without dispersed graphene. Samples were prepared at an initial concentration of 1.5 mg ml^{-1}, after 15 minutes sonication time followed by two rounds of 7.5 minute centrifugation at 7000 rpm. b) Picture showing the stability of the graphene dispersions after one month, with additional images of Cyrene dispersions after 1 month prepared with various sonication times (same initial concentration of 1.5 mg ml^{-1}).

Surface tension study. The relationship between the contact angles (Figure S3) and the surface energy of the graphene monolayer on Si/SiO_2 can be expressed by Equation 1, which is derived from Young's equation and the work of adhesion of liquids in solid surfaces and applying the Neumann's equation of state theory.[5] In Equation 1, β is the constant coefficient of graphene.

$$ln\left[\delta_{sol}\left(\frac{1+cos\theta}{2}\right)^2\right] = -2\beta(\delta_G - \delta_{sol})^2 + \ln(\delta_G) \qquad \text{Eq. (1)}$$

A plot of the left-hand side of the Equation 1 as a function of the solvent surface energy (δ_{sol}) was fitted with a second-order polynomial curve, from which β and the surface tension of graphene on SiO_2 can be determined (δ_G). A good fit of the experimental points (excluding triacetin) was obtained (Figure S4).

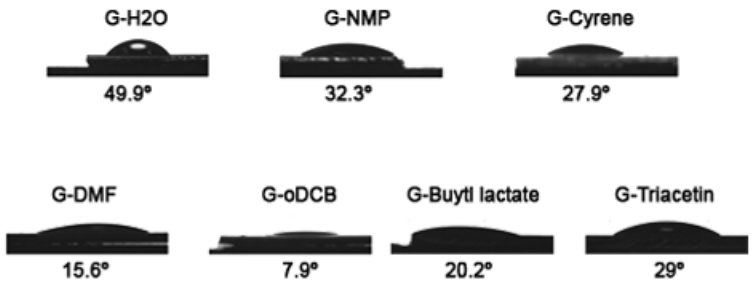

Figure S3. Contact angle study for the verification of graphene affinity on CVD-graphene monolayer on Si/SiO_2.

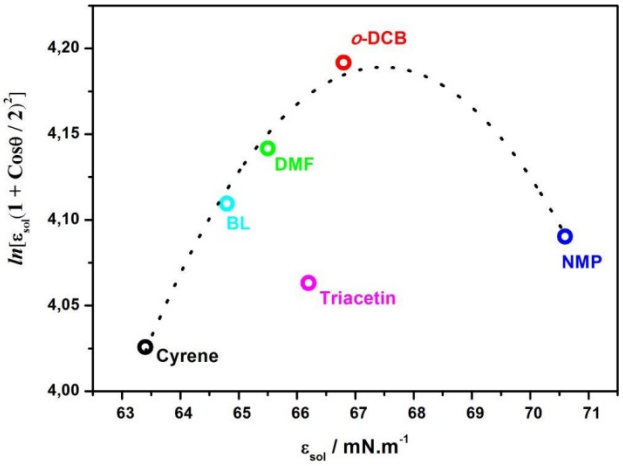

Figure S4. Calculation of the graphene surface energy. Variation of contact angle with solvent's surface energy according to Neumann's equation including triacetin.

High solvent affinity for the graphene surface manifests itself through the wettability of the solvent and a low contact angle.[5] The tension at this solid-liquid interface is a result of attractive intermolecular forces. If the interfacial tension between the surface and the solvent is low then there will be little enthalpy loss in creating the surface-solvent interface, hence minimizing the energy cost of exfoliation. The lowest contact angles, and subsequently the best wetting performances, are observed for solvents with a surface tension between 35 mN m^{-1} and 38 mN m^{-1}, corresponding to *o*DCB and DMF. As anticipated from the higher graphene concentration in Cyrene in relation to NMP, the contact angle formed by Cyrene was found to be lower than that for NMP, but only marginally. Considering all the organic solvents, the surface energy value of the graphene employed was calculated to be 67 mN m^{-1} using Neumann's equation of state theory, in excellent agreement with previous findings.[6]

It has been previously demonstrated that the contact angle of water droplets on graphene depends on the number of layers,[7,8] the substrate,[9] and the duration of the experiment, which can be affected through the absorption of airborne contaminates, including hydrocarbons.[10] Although in our study we are also using a range of organic solvents, we have considered these variables. In summary the time dependence is controlled by collecting the contact angle values immediately after depositing the drop of solvent. The thickness and

uniformity of the CVD-graphene were evaluated by Raman spectroscopy. The I_{2D}/I_G intensity ratio and the full width at half-maximum of the 2D band, related to the number of CVD-graphene layers, are 1.7 ± 0.2 and 36.9 ± 0.8 cm^{-1} respectively, resembling the values previously observed for CVD-graphene.[11,12] This data is indicative of graphene uniformly distributed on the Si/SiO_2 surface, allowing us to discard the effect of the graphene thickness on the contact angles. Moreover, reference experiments of contact angles on Si/SiO_2 wafers (without graphene) were conducted to evaluate the influence of the substrate. The measured values were very similar for all organic solvents (~32.0º to 36.6º) demonstrating minimal influence of the Si/SiO_2 substrate on the contact angle.

High resolution transmission electrion microscopy. Lower magnification images of the dispersions were taken as an initial assessment of the quality of the graphene flakes, and also aid with the measurement of the lateral flake dimensions. It can be seen in Figure S5, images A and B (Cyrene) that the flakes are much better dispersed in comparison to the flakes seen in images E and F for NMP, which by comparison are much more agglomerated. This is clearer when comparing images in Figure S5 C and D with those in Figure S5 G and H, where the latter are overall larger, but from their representative diffraction patterns are observed to be multilayer to graphitic. The flakes formed in Cyrene are bi- to few layers. Figure S6, images A-D, show HRTEM images of various flakes with well-defined edges, ranging from probable single layer graphene to few layer graphene produced from the Cyrene graphene dispersion. Images E-H are for those obtained from the NMP-graphene dispersion, and as can be seen they range from few layer flakes to graphitic particles in nature. Additionally, when comparing the lateral dimensions of the samples prepared in either Cyrene or NMP it can be seen that for flake sizes with ≤10 layers, flakes produced using Cyrene are actually larger on the whole (see Figure S7).

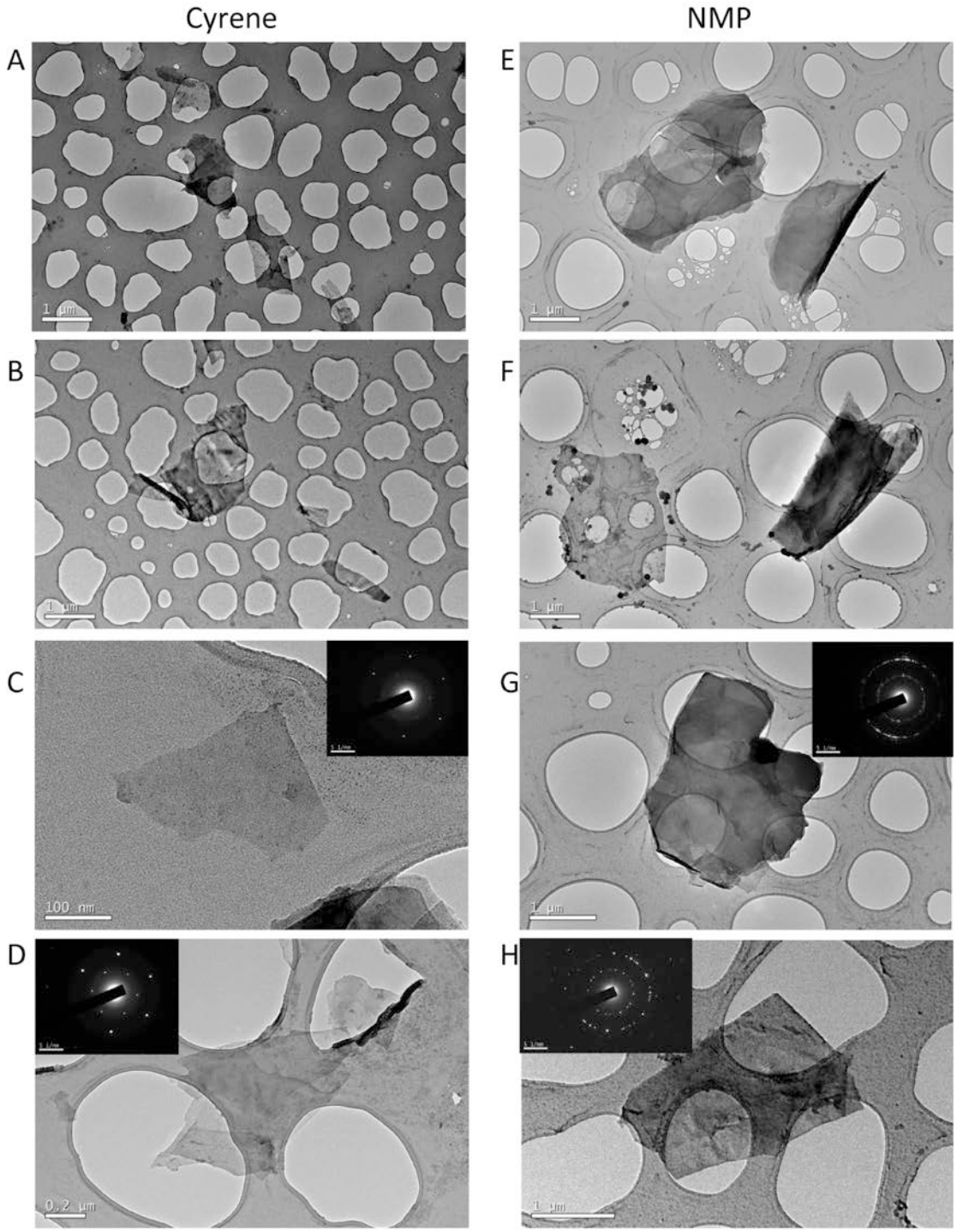

Figure S5. High resolution transmission electron microscopy (HRTEM) of graphene produced in Cyrene and NMP. Lower magnification TEM images of dispersions achieved with Cyrene (inset images A and B) and NMP (E and F). High magnification images of flakes with various layers can be seen in images C and D (Cyrene) and G and H (NMP).

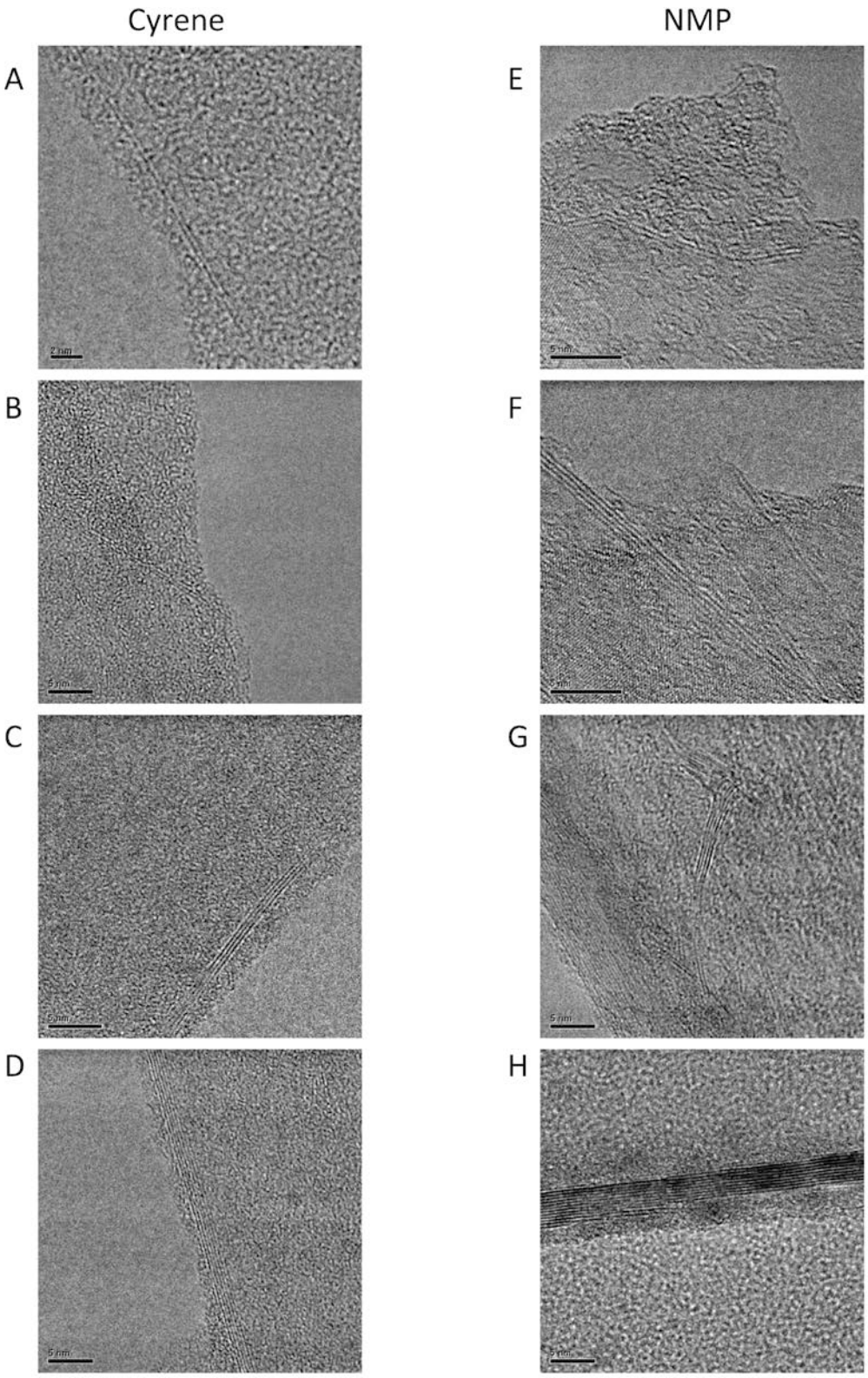

Figure S6. HRTEM images showing the edges of Cyrene dispersed graphene (inset images A-D) and NMP dispersed graphene (E-H).

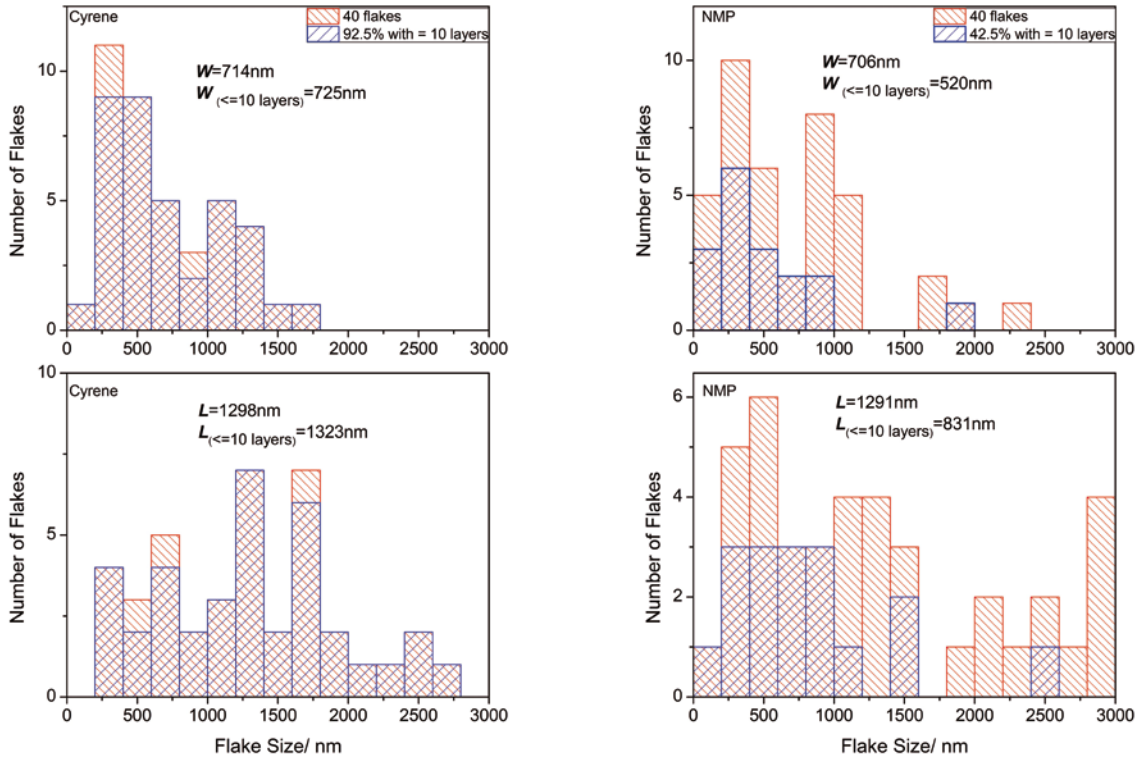

Figure S7. Flake length (L) and width (W) dimensions taken from TEM measurements for both Cyrene (left) and NMP (right) dispersions.

Raman graphene quality analysis. Examination of the Raman 2D band in this work was found to be very instructive in ruling out whether the postulated 'protection' offered by viscous solvents counteracts the critical role of surface tension. It is accepted that the number of Lorentzian curves (FWHM ~ 24) making up the 2D band relates to the number of stacked graphene layers.[13-15] Here deconvolution of 2D Raman band for Cyrene suggested the formation of polydisperse samples ranging from two to a few and multilayers graphene, similar to NMP treated under the same conditions (Figure S8). Furthermore, the 2D band width, another parameter used to determine the thickness of graphene laminates, is very similar for both samples, which also suggests that they represent a similar thickness of graphene.[16] The difference between this and the results of TEM *etc*. are due to the extended drying times of the dispersion on the Si/SiO_2 wafer in comparison to the holey carbon grid used for TEM and also the fact that monolayer graphene is virtually invisible under an optical

microscope to be able to locate them and test them, even when using recommended Si/SiO_2 (300 nm).

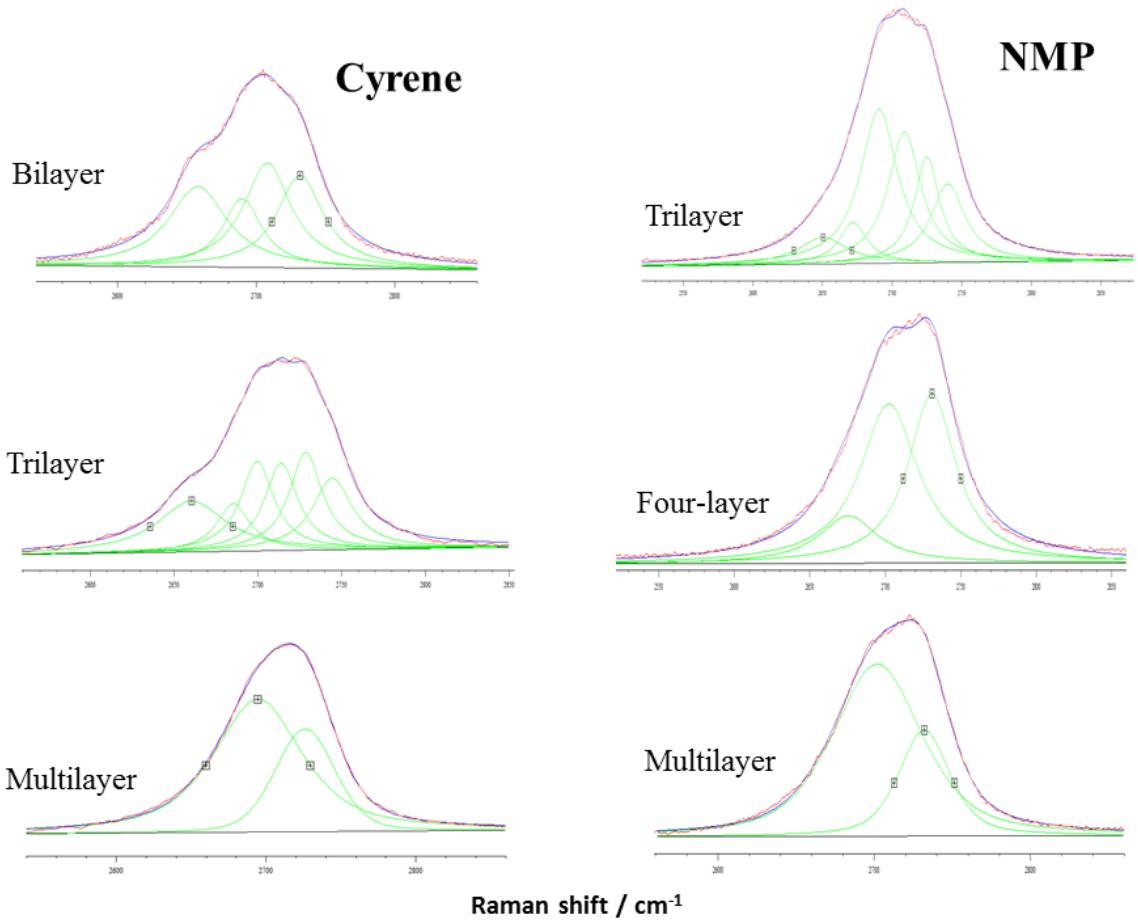

Figure S8. Raman 2D band deconvolution to estimate the number of graphene stacked layers. The spectra were acquired in different points of samples deposited by drop-casting on Si/SiO_2 substrates.

A general expression to estimate the crystallite size L_a from the integrated intensity ratio I_D/ I_G has been proposed by Cançado *et al.*,[17] and can be written as follows (Equation 2) where λ is the laser wavelength in nm, in this case 514 nm.

$$L_a(nm) = 2.4x10^{-10}\lambda_l^4\left(\frac{I_D}{I_G}\right)^{-1} \qquad \text{Eq. (2)}$$

The distance between defects (L_D) and the defect density (n_D) can also be estimated from the I_D/ I_G using experimentally determined equations.[18] The L_D can be written as is shown in Equation 3, and the density of defect as Equation 4.

$$L_D^2(nm^2) = (1.8 \pm 0.5) \times 10^{-9} \lambda_l^4 \left(\frac{I_D}{I_G}\right)^{-1} \quad \text{Eq. (3)}$$

$$n_D(cm^{-2}) = \frac{(1.8 \pm 0.5) \times 10^{22}}{\lambda_l^4} \left(\frac{I_D}{I_G}\right) \quad \text{Eq. (4)}$$

Changes in L_a, L_D, and the defect density (n_D) compared with the viscosity of the tested solvents are shown in Figure S9.

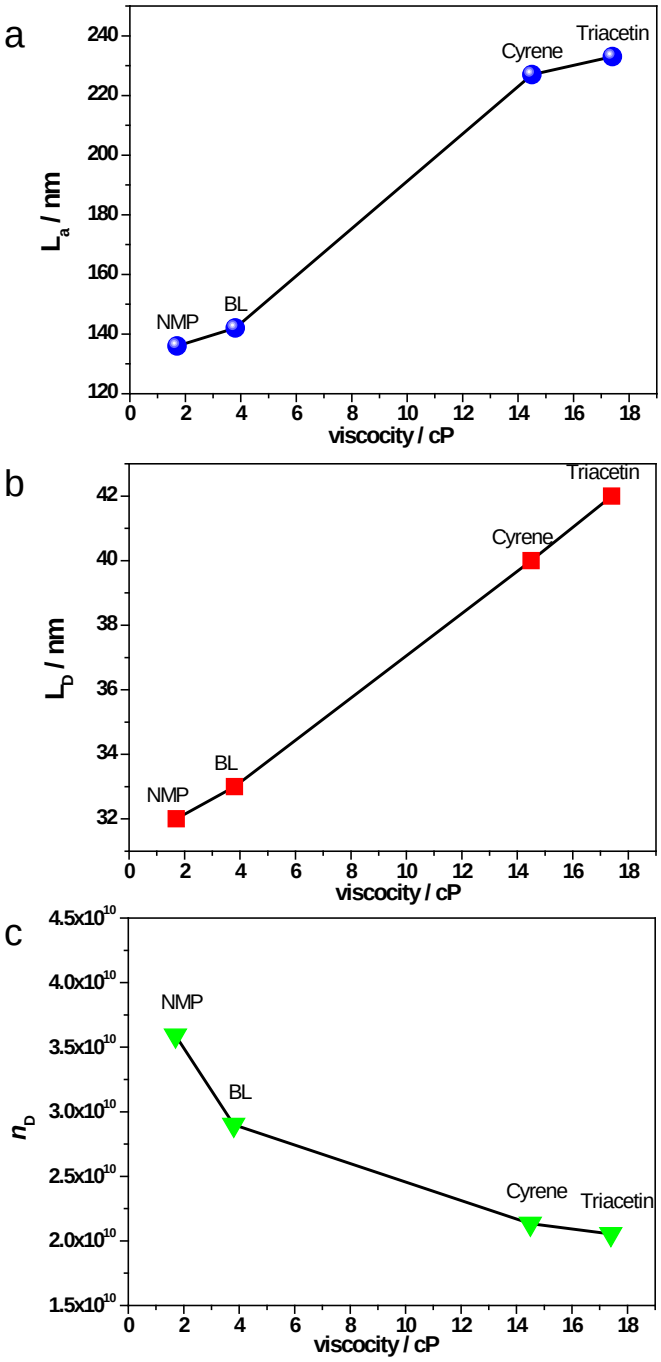

Figure S9. Variation in characteristic parameters of graphene flakes, obtained from the I_D/I_G Raman ratio. A) Crystallite size, L_a; B) distance between defects (L_D); and, C) the density of defects (n_D). The viscosity of the tested solvents increases in the following order: NMP, Cyrene, and triacetin.

The evaluated parameters display an apparent relationship with solvent viscosity. As expected, the flakes obtained in solvents with higher viscosity display larger graphitic domains and lower density of defects. Although solvents of intermediate viscosity need to be

tested to appropriately obtain an equation describing the variation of each parameter with viscosity, the data in Figure S9 clearly demonstrates the effect of viscosity on the structural integrity of graphene flakes.

Exfoliation optimization. The experimental parameters, e.g. sonication time and initial graphite concentration that determine the concentration of the dispersed graphene were re-evaluated. Long sonication times have previously been reported as a means to obtain high graphene concentrations in NMP.[19] This this may also be advantageous for dispersions in Cyrene. The aim of our investigation here was to establish the optimal conditions that maximize the dispersion of graphene for commercially pertinent applications, whilst preserving the structural integrity of the graphene flakes.

Firstly, different initial concentrations of graphite, C_i, of 0.5, 1.5, 5.0 and 10 mg mL^{-1} were tested to evaluate the exfoliation of graphite to dispersed graphene in Cyrene (Figure S10a). The amount of dispersed material was determined by UV-visible spectroscopy, where the absorbance at 660 nm was measured in the same way as previously outlined. An almost linear dependence of the amount of dispersed graphene versus the starting graphite amount was observed up to C_i = 5 mg mL^{-1}, with the gradient accounting for an additional 0.15 mg of dispersed particles for every 1 mg increase in the starting graphite loading. Few gains are made beyond an initial graphite concentration of 5 mg mL^{-1}, but still graphene concentrations of ~1 mg mL^{-1} can be reached with an initial graphite load of C_i = 10 mg mL^{-1}. Figure S10b presents the percentage of the initial graphite that can be converted into dispersed particles. It is evident that this quantity initially increases, reaching a maximum (16%) in the range 1.5 mg mL^{-1} < C_i < 5 mg mL^{-1} and then decreases significantly to no more than 10% when C_i = 10 mg mL^{-1}. This trend can be related to the effect of powdered graphite particles on the efficiency of sonication, and consequently exfoliation. Specifically, high amounts of

suspended graphite powder minimize the efficiency of the ultrasound irradiation leading to less particles being able to benefit from the desired cavitation phenomenon.[20]

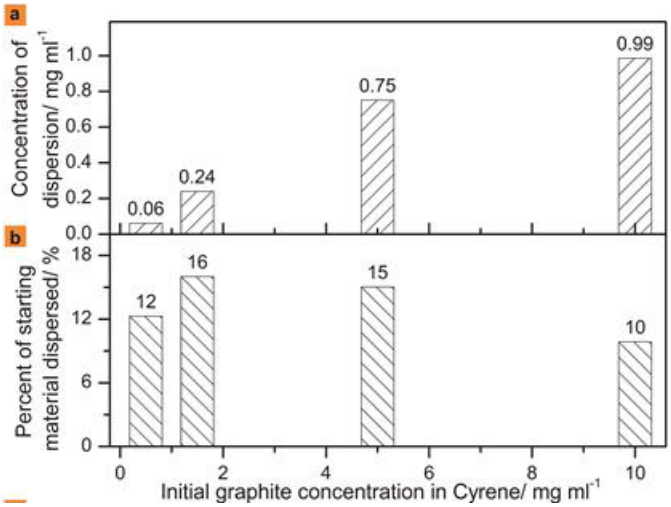

Figure S10. Graphene dispersion parameter optimization. a) Variation of the initial graphite concentration versus the measured the concentration of graphene dispersed after the standard 15 minutes sonication and 10 minutes centrifugation, and, b) the respective percentage of starting graphite that in-turn converts to dispersed graphene.

Solvent selection procedure

Overview. A solvent selection protocol was developed to identify ideal solvents for graphene processing and to help define the precise role of the solvent. Given the clearly recognisable need, the methodology was developed to find a high performance yet green solvent. Algorithms for solvent selection have been used previously to optimise the solvent for simple extractions, and in examples of reaction chemistry.[21] If the requirements of the solvent can be defined in terms of measurable properties, then we postulated that the principle can also be applied to the more complex problem of graphite exfoliation and the subsequent dispersion of graphene flakes in solution. There has been much debate over the exact role of the solvent in the processing of carbon nanostructures,[22-25] which is not fully understood. Nevertheless there is a consensus that solvent surface energy and viscosity are both crucially important in order to achieve an acceptable concentration of dispersed graphene.[3,25] The polarity of the medium is also influential, and Hansen solubility parameters have been used previously to correlate graphene concentration to solvent polarity.[26,27] However different reports do not always agree on the significance of each solvent property, or in some instances what the ideal value of that property actually is.[3,5] That being the case, an approach to solvent selection that can be easily updated, added to, or otherwise modified is greatly beneficial.

Here we report a high throughput screening of a large database of solvents in order to identify green solvents able to disperse graphene in relatively high concentrations. After a comprehensive selection process, the most promising solvent candidates, as indicated through calculation, were subjected to an experimental validation of their performance. This multi-stage assessment of solvent properties was designed to refine a large solvent dataset, far beyond the number of solvents that could actually be tested experimentally, to only the environmentally friendly solvent candidates with an anticipated high performance. This is a

key difference between this approach and the solely experimental methods of other studies that make use of Hansen solubility parameters.[26] A series of experiments and analysis confirmed the theoretical predictions, with Cyrene for example achieving highly concentrated dispersions of quality graphene flakes.

To the best of the authors' knowledge, this work is the first attempt to select a solvent for creating graphene dispersions by considering relevant properties in a logical, systematic way, but crucially without the restriction of choosing a solvent from a small experimental set. The approach employed reduces a large number of possible solvent candidates to a shortlist consisting of only those solvents that meet the requirements of each criterion. Thus, experimental validation of the solvent selection protocol is only required for a minimal number of solvents, thus creating a streamlined investigation that at the same time actually encompasses several hundreds of solvents more than a typical, experimentally led project. The act of carrying out the solvent selection process creates a better understanding of the relevant solvent characteristics. This in turn assists with future solvent development, where the solvent selection process may be adapted or new solvent candidates introduced in later iterations. A concise version of the assessment is provided as a separate (Microsoft Excel) file.

The first round of the methodology concerns the solvent properties that influence the performance of the process (*i.e.* ultrasound assisted exfoliation and graphene dispersion). A polarity matching exercise using Hansen solubility parameters established suitable solvents on the basis of bulk solution interactions with graphene. Target parameters representing the polarity of graphene were obtained from the literature.[26] Secondly the interaction between the solvent and graphene through their surface energies, again relevant to exfoliation and dispersion stability, was also used to select promising solvent candidates.[5,6] Finally the stability of a graphene suspension was approximated using Stokes' law of settling velocities,

where the density/viscosity ratio is important (as explained subsequently). The three criteria were applied in individual assessments, not sequentially (Table S1). This is so that if a requirement is changed, the recalculation of the solvent shortlist is simplified. Solvent candidates move through to the next stage of the assessment only if they meet the requirements of all three parallel performance criteria.

Table S1. Solvent selection performance criteria.

Performance metric	**Measurement**	**Target**	**Requirement**
Solvent-solute interaction	Polarity (calculated)	δ_D = 18 $MPa^{0.5}$ δ_P = 9.3 $MPa^{0.5}$ δ_H = 7.7 $MPa^{0.5}$	Hansen distance between target and solvent lower than 6.5 $MPa^{0.5}$.
Solvent-solute interaction	Surface tension	$\gamma = 38.2 \pm 6$ $mN \cdot m^{-1}$	Solvent surface tension falls within designated range.
Dispersion stability	Density (ρ / $g \cdot mL^{-1}$) and dynamic viscosity (μ / $g \cdot s^{-1} \cdot m^{-1}$)	$\rho/\mu \leq 1.20\ 10^6$ $s \cdot m^{-2}$	Low density/viscosity ratio.

The original dataset of solvents exceeded 10,000 entries. The large number of solvent candidates was processed using the HSPiP solubility estimation software package, sorting by polarity. The remaining data analysis was performed in a spreadsheet (refer to the separate electronic supplementary information file). Many of the solvents contained in the dataset lack experimental viscosity and surface tension data, meaning they cannot pass all the solvent selection criteria for this reason alone. However this exercise does highlight promising solvents that could be synthesised and their additional physical properties tested. Computational estimates could also guide this task and future work will investigate this possibility further. The original HSPiP dataset from which the list of solvent candidates was derived was supplemented by a number of bio-based solvents, to which special interest was

paid within the assessment (Table S2). A summary of how each bio-based solvent fared during the solvent selection process is maintained throughout the following discussions.

Table S2. Bio-based solvents included in the solvent selection process.

Solvent name	Bio-based content*	Source[§]
1,2-Pentanediol	100%	Pyrolysis of carbohydrate
1,2-Propanediol	100%	Derived from glicerol
1,3-Propanediol	100%	Derived from glicerol
1,4-Butanediol	100%	Fermentation product
1-Butanol	100%	Fermentation product
2-Butanol	100%	Fermentation product
2-Methyltetrahydrofuran	100%	Pyrolysis of carbohydrate
2-Octanol	100%	Synthesised from vegetable oils
2-Propanol	100%	Fermentation product
Acetic acid	100%	Fermentation product
Acetone	100%	Fermentation product
Acetyltributyl citrate	18%	Made from citric acid
Butyl lactate	43%	Made from lactic acid
Butyric acid	100%	Fermentation product
Cyrene	100%	Pyrolysis of carbohydrate

Table S2. Bio-based solvents included in the solvent selection process. (continued).

Solvent name	Bio-based content*	Source[§]
Diethoxymethane	80%	Made with bio-ethanol
Dimethyl ether	100%	Made from bio-gas
Dimethyl isosorbide	75%	Pyrolysis of carbohydrate
Dimethyl sulphoxide	100%	Made from dimethyl sulphide
d-Limonene	100%	Essential oils

Ethanol	100%	Fermentation product
Ethyl acetate	100%	Made from bio-ethanol
Ethyl lactate	100%	Made from lactic acid
Ethylene glycol	100%	Made from bio-ethanol
Eugenol	100%	Essential oils
Furfural	100%	Pyrolysis of carbohydrate
Furfuryl alcohol	100%	Pyrolysis of carbohydrate
Glycerol	100%	Vegetable oils
Glycerol carbonate	75%	Derived from glicerol
Glycerol formal	75%	Derived from glicerol
Isoamyl alcohol	100%	Fermentation product
Isobutanol	100%	Fermentation product
Isoeugenol	100%	Essential oils
Lactic acid	100%	Fermentation product
Lauric acid	100%	Vegetable oils
Levulinic acid	100%	Pyrolysis of carbohydrate
Methanol	100%	Made from bio-gas
Methyl lactate	75%	Made from lactic acid
Methyl oleate	95%	Synthesised from vegetable oils

Table S2. Bio-based solvents included in the solvent selection process. (continued).

Solvent name	**Bio-based content***	**Source**[§]
Oleic acid	100%	Vegetable oils
p-Cymene	100%	Made from limonene
Solketal	50%	Derived from glicerol
t-Butyl ethyl ether	33%	Made with bio-ethanol
Tetrahydrofuran	100%	Pyrolysis of carbohydrate
Tetrahydrofurfuryl alcohol	100%	Pyrolysis of carbohydrate

Triacetin	33%	Derived from glicerol
Triethyl citrate	100%	Made from citric acid
α-Pinene	100%	Essential oils
α-Terpineol	100%	Essential oils
β-Pinene	200%	Essential oils
γ-Valerolactone	100%	Pyrolysis of carbohydrate

**Bio-based content is calculated on the basis of the number of carbon atoms from biomass origin as a percentage of the total carbon content.*

[§]*References are provided in the supplementary excel file.*

The second phase of the solvent selection process rejects solvents with obvious environmental, health and safety (EHS) issues under scrutiny by legislation. The first of these requirements is that no solvent possesses known carcinogen, mutagen, or reprotoxic (CMR) characteristics. This is supplemented with an acute toxicity assessment, for these solvents should also be avoided where possible (Table S3). Then the environmental persistency, bioaccumulation, and toxicity (PBT) of solvents meeting the performance criteria was considered. These health and environmental requirements are implemented in the solvent selection process according to the requirements of the EU regulation (EC) No 1907/2006, Registration, Evaluation, Authorisation & restriction of CHemicals (REACH) and the EU regulation (EC) No 1272/2008, Classification, Labelling and Packaging (CLP). It is important to align the requirements of each criteria to formal legislated property values in order to be industrially and commercially relevant. Arbitrary thresholds have been avoided so not to introduce a preference or inadvertent bias for a particular solvent.

Table S3. Solvent selection legislative criteria.

EHS metric	Indicator	Requirement
CMR or acutely toxic		

Acute toxicity	H300, H301, H310, H311, H330, or H331 hazard statements*	LD_{50} >300 mg/kg (avoiding CLP category 1, 2, or 3: fatal/toxic).
Carcinogenic	Carcinogenicity category 1A, 1B, or 2*	Neither a category 1 or 2 carcinogen (REACH).
Mutagenic	Germ cell mutagenicity categories 1A, 1B, or 2*	No evidence of mutagenicity (REACH), including animal trials and Ames test.
Reproductive toxin	Reproductive toxicity categories 1A, 1B, or 2*	Neither a category 1 or 2 reproductive toxicant (REACH).
*PBT***		
Persistent	Biodegradation (multiple test methods and calculations available).	Solvent must be considered as biodegradable.
Bioaccumulating	logP	logP < 4 indicates potential to bioaccumulate (CLP).
Toxic	EC_{50}	EC_{10} > 0.01 mg/L (REACH).

**The associated hazard statements are defined in the EU CLP directive (Regulation No. 1272/2008).*

***All three categories must apply for a substance to be considered PBT, but for this assessment each category is considered individually.*

Solvent candidates meeting the performance criteria and also found to have suitable EHS profiles formed a final shortlist, and were then ranked according to additional criteria describing the greenness of each solvent. The topic of greenness is highly subjective, and this is an undesirable approach when making an assessment. Therefore solvents were just compared in this respect, and not selected or rejected on the basis of any green chemistry principles. Indicators of greenness were chosen that could be discussed and compared in the context of regulation (Table S4). No thresholds were set, although ideal target values derived from legislation are suggested to help identify the most promising of candidates. European regulation (EC) 1272/2008 on classification, labelling and packaging of substances and mixtures (CLP) and European Directive 2010/75/EU (industrial emissions directive) are both helpful in this respect. The toxicity threshold values are larger than what were used in the

EHS criteria, broadened out to include less severe hazards, yet still requiring labelling according to the CLP directive. In addition, bio-based solvents made from renewable resources were prioritised, under the guidance of European Technical Specification TS/16766.[28] This process helped to identify butyl lactate, Cyrene, and triacetin as the primary candidates for the sustainable solvent processing of graphene, incorporating practical, regulatory, environmental, health, and safety aspects as part of this judgement. Greater detail on each of these assessment phases is now provided. A spreadsheet containing the solvent selection calculations has also been made available for greater detail.

Table S4. Solvent selection greenness criteria.

Greenness criteria	Target or threshold value	Justification and context
Renewability		
Bio-based content	≥25%	Minimum of 25% bio-based carbon content (as proportion of total carbon content) given in European technical specification TS/16766,entitled *Bio-based solvents: Requirements and test methods* to qualify as a bio-based product.
Toxicity		
LD_{50} (rat, oral)	> 2000 $mg \cdot kg^{-1}$	'Acute toxicity' threshold, below which a substance is recognised as harmful (European regulation (EC) 1272/2008, CLP).
Flammability		
Autoignition temperature	None set.	Indicative of safety. No threshold listed in the CLP regulation.
Flash point	> 60 °C	'Flammable liquids' threshold (CLP).
Environmental impact		
Vapour pressure	< 0.075 mmHg	Industrial emissions 'VOC' threshold (European directive 2010/75/EU).
logP	< 4	'Harmful to the aquatic environment' threshold (CLP), applied in combination with EC_{50}.
EC_{50} (Daphnia magna, 48 hours)	> 100 $mg \cdot L^{-1}$	'Harmful to the aquatic environment' threshold (CLP), applied in combination with logP.
Biodegradability	None set.	Indicative of persistence.

Hansen solubility. The Hansen solubility parameters were originally established as an empirical description of polymer solubility.[29] However they are now widely used to identify solvents for a wide range of solutes, including carbon nanostructures.[5,30-32] In Hansen solubility theory, solutes are predicted to be most soluble in solvents with a similar polarity, as defined by three scales describing dispersion forces (δ_D), dipole forces (δ_P), and hydrogen

bonding interactions (δ_H). The length of a vector connecting a solvent to a solute in this three dimensional Hansen space is indicative of the likely solubility. Using characteristic values for graphene ($\delta_D \sim 18.0$ MPa$^{1/2}$; $\delta_P \sim 9.3$ MPa$^{1/2}$; $\delta_H \sim 7.7$ MPa$^{1/2}$),[26] potential solvents can be found computationally. The Hansen parameters are typically calculated rather than obtained from experiments, so the potential solvent set is infinite. This equally applies to theoretical solvent structures before they are first synthesised. Using the *Hansen Solubility Parameters in Practice* (HSPiP) software, a number of potential graphene dispersing solvents were identified from more than 10,000 candidates contained within the software. As stated earlier, this dataset was complimented with 51 bio-based solvent entries taken from the University of York's *Sustainable Solvent Selection Service* (S4) database.

A representative selection of solvents is shown in the following polarity diagram to demonstrate the solvent selection process (Figure S11). The assignment of solvents and non-solvents, and hence the boundary of the so-called solubility sphere (shown in green) was defined using a minimal number of experimental observations already available in the literature. While acetone is seen as a poor solvent for graphene dispersibility,[26] it is actually a better polarity match to graphene in the 3D Hansen space (radius of 5.2 MPa$^{0.5}$) than DMF (5.8 MPa$^{0.5}$), the latter being a recognised solvent. This suggests other solvent properties are relevant. A sphere radius of 6.5 MPa$^{0.5}$ was chosen to differentiate between potentially suitable and unsuitable solvents on the basis of polarity (Figure S11). Acetone and DMF are both contained within this boundary.

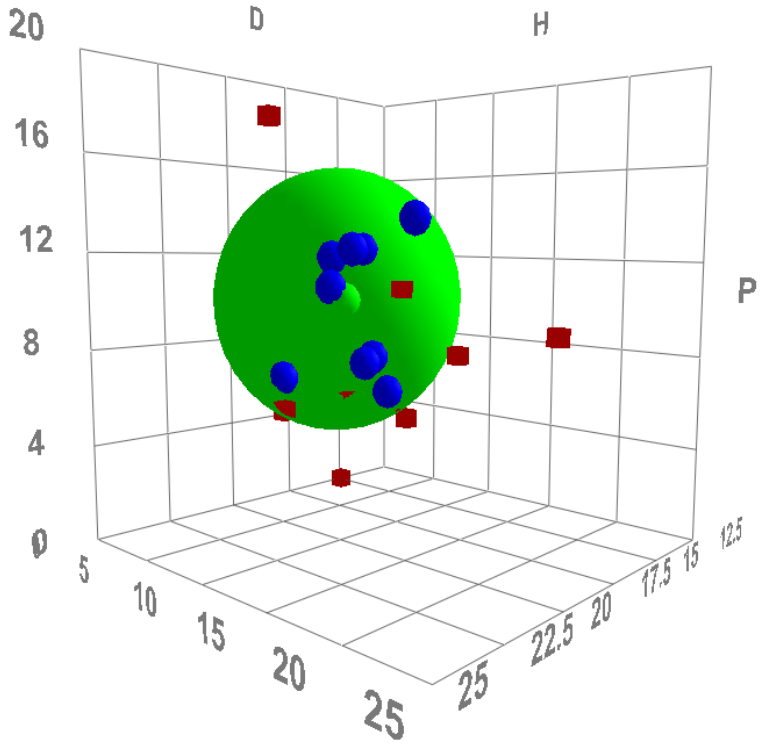

Figure S11. A three dimensional Hansen solubility map, where graphene is shown as the green data point, some representative solvents as solid blue data points, and a selection of non-solvents shown as red data points. The green sphere marks the boundary between solvents and non-solvents as calculated by the HSPiP software.

From this analysis a great number of solvent candidates can be ruled out because of their unsuitable polarity. From the original solvent set, more than 4000 compounds were identified has having a desirable polarity, and retained for further consideration. Note that the other two performance criteria rely on experimental data (*i.e.* density/viscosity and surface tension), and so a great deal of the solvents identified on the basis of their polarity cannot continue onwards through the solvent selection process. However very good polarity matches could always warrant experimental determination of these physical properties in the search for alternative solvents, although this was not pursued at this time.

Most of the 51 bio-based solvents in the original dataset do not possess the desired polarity. Only 18 met this requirement (Table S5), of which the closest polarity match to graphene was Cyrene (dihydrolevoglucosenone), followed by dimethyl isosorbide. Prominent

bio-based solvents with an undesirable polarity, and thus eliminated from the assessment, included limonene, ethanol, and glycerol.

Table S5. Polarity characteristics of the bio-based solvents.

Solvent name	δ_D /MPa^{½}	δ_P /MPa^{½}	δ_H /MPa^{½}	Radius	Status
1,2-Pentanediol	16.7	7.2	16.8	9.69	Fail
1,2-Propanediol	16.8	10.4	21.3	13.9	Fail
1,3-Propanediol	16.8	13.5	23.2	16.2	Fail
1,4-Butanediol	16.6	11.0	20.9	13.6	Fail
1-Butanol	16.0	5.7	15.8	9.72	Fail
2-Butanol	15.8	5.7	14.5	8.86	Fail
2-Methyltetrahydrofuran	16.9	5.0	4.3	5.91	Pass
2-Octanol	16.1	4.2	9.1	6.51	Fail
2-Propanol	15.8	6.1	16.4	10.3	Fail
Acetic acid	14.5	8.0	13.5	9.18	Fail
Acetone	15.5	10.4	7.0	5.17	Pass
Acetyltributyl citrate	16.7	2.5	7.4	7.29	Fail
Butyl lactate	15.8	6.5	10.2	5.78	Pass
Butyric acid	15.7	4.8	12.0	7.74	Fail
Cyrene	18.8	10.6	6.9	2.21	Pass
Diethoxymethane	15.4	5.7	5.1	6.84	Fail

Table S5. Polarity characteristics of the bio-based solvents. (continued).

Solvent name	δ_D /MPa^{½}	δ_P /MPa^{½}	δ_H /MPa^{½}	Radius	Status
Dimethyl isosorbide	17.6	7.1	7.5	2.35	Pass
Dimethyl sulphoxide	18.4	16.4	10.2	7.57	Fail
d-Limonene	17.2	1.8	4.3	8.39	Fail

Ethanol	15.8	8.8	19.4	12.5	Fail
Ethyl acetate	15.8	5.3	7.2	5.97	Pass
Ethyl lactate	16	7.6	12.5	6.48	Pass
Ethylene glycol	17.0	11.0	26.0	18.5	Fail
Eugenol	19.0	7.5	13.0	5.94	Pass
Furfural	18.6	14.9	5.1	6.29	Pass
Furfuryl alcohol	17.4	7.6	15.1	7.69	Fail
Glycerol	17.4	11.3	27.2	19.6	Fail
Glycerol carbonate	17.9	25.5	17.4	18.9	Fail
Glycerol formal	18.4	10.6	16.5	8.93	Fail
Isoamyl alcohol	15.8	5.2	13.3	8.22	Fail
Isobutanol	15.1	5.7	15.9	10.7	Fail
Isoeugenol	18.9	5.7	9.9	4.59	Pass
Lactic acid	17.3	10.1	23.3	15.7	Fail
Lauric acid	16.2	4.1	7.4	6.33	Pass
Levulinic acid	17.1	10.4	13.5	6.17	Pass
Methanol	14.7	12.3	22.3	16.3	Fail
Methyl lactate	16.9	8.3	16.1	8.74	Fail
Methyl oleate	16.2	3.8	4.5	7.31	Fail
Oleic acid	16.0	2.8	6.2	7.78	Fail
p-Cymene	17.3	2.4	2.4	8.81	Fail

Table S5. Polarity characteristics of the bio-based solvents. (continued).

Solvent name	**δ_D /MPa^{½}**	**δ_P /MPa^{½}**	**δ_H /MPa^{½}**	**Radius**	**Status**
Solketal	16.6	7.9	12.0	5.32	Pass
t-Butyl ethyl ether	14.4	3.5	2.7	10.5	Fail
Tetrahydrofuran	16.8	5.7	8.0	4.34	Pass
Tetrahydrofurfuryl alcohol	17.8	8.2	12.9	5.33	Pass

Triacetin	16.5	4.5	9.1	5.83	Pass
Triethyl citrate	16.5	4.9	12	6.84	Fail
α-Pinene	16.4	1.1	2.2	10.4	Fail
α-Terpineol	17.1	3.6	7.6	5.98	Pass
β-Pinene	16.3	1.1	1.9	10.6	Fail
γ-Valerolactone	16.9	11.5	6.3	3.41	Pass

Surface energy. Only eleven of the bio-based solvents pass the surface tension requirement, and 53 in total (Table S6). No surface tension data for γ-valerolactone was available, but considering its successful progress in other aspects of the solvent selection process it was important in this case to have an idea of its surface tension through computational estimates. Using HSPiP, the surface tension of γ-valerolactone was calculated to be unsatisfactory (29.9 mN m^{-1}). The same applies for dimethyl isosorbide. Experimental testing of these two promising solvents should be considered in future studies. Six bio-based solvents pass the requirements for both the polarity and the surface tension criteria: butyl lactate, Cyrene, furfural, levulinic acid, tetrahydrofurfuryl alcohol and triacetin.

Table S6. Surface tension characteristics of the bio-based solvents.

Solvent name	**Surface tension /mN m^{-1}**	**Status**
1,2-Pentanediol		No data
1,2-Propanediol	40.1	Pass
1,3-Propanediol		No data
1,4-Butanediol	44.6	Fail
1-Butanol	24.7	Fail

2-Butanol	23.4	Fail
2-Methyltetrahydrofuran		No data
2-Octanol	26.4	Fail
2-Propanol	20.9	Fail
Acetic acid	27.4	Fail
Acetone	22.7	Fail
Acetyltributyl citrate		No data
Butyl lactate	35.0	Pass
Butyric acid	26.7	Fail
Cyrene	33.6	Pass
Diethoxymethane	21.6	Fail
Dimethyl ether	16.0	Fail
Dimethyl isosorbide		(Fail)*
Dimethyl sulphoxide	43.0	Pass
d-Limonene	26.9	Fail

Table S6. Surface tension characteristics of the bio-based solvents. (continued).

Solvent name	**Surface tension /mN m^{-1}**	**Status**
Ethanol	21.2	Fail
Ethyl acetate	23.8	Fail
Ethyl lactate	29.2	Fail
Ethylene glycol	48.5	Fail
Eugenol	30.9	Fail
Furfural	43.5	Pass

Furfuryl alcohol	38.0	Pass
Glycerol	63.4	Fail
Glycerol carbonate		No data
Glycerol formal	44.5	Fail
Isoamyl alcohol	23.8	Fail
Isobutanol	23.0	Fail
Isoeugenol	30.8	Fail
Lactic acid		No data
Lauric acid	26.6	Fail
Levulinic acid	39.7	Pass
Methanol	22.3	Fail
Methyl lactate	39.0	Pass
Methyl oleate	31.3	Fail
Oleic acid	32.8	Pass

Table S6. Surface tension characteristics of the bio-based solvents. (continued).

Solvent name	**Surface tension /mN m^{-1}**	**Status**
p-Cymene	28.1	Fail
Solketal	32.1	Fail
t-Butyl ethyl ether	19.1	Fail
Tetrahydrofuran	26.4	Fail
Tetrahydrofurfuryl alcohol	37.0	Pass
Triacetin	35.5	Pass
Triethyl citrate		No data

α-Pinene	25.9	Fail
α-Terpineol	31.6	Fail
β-Pinene	26.9	Fail
γ-Valerolactone		(Fail)*

**No experimental data was available. The calculated surface tension did not meet the requirement.*

Viscosity. At this point it is worth emphasising that polarity (a thermodynamic trait) is not the only solvent property responsible for solubility. Kinetic factors are also applicable. The frictional forces present between solvent and solute, and the resulting settling velocity when establishing the suspension of graphene particles are likely to influence the concentration and stability of the dispersion. Although applied for spherical particles, we assume here that Stokes' law can also be used in this instance (*i.e.* for flat laminates).[33] According to Stokes' law, the settling velocity under centrifugation is given by equation 5:

$$V_s = \frac{8}{9} \frac{r_g^2 \pi^2 f^2 R(\rho_g - \rho_s)}{\mu} \qquad \text{Eq. (5)}$$

Most of the variables relate to the particles, with r_g representing the lateral average size of graphene flakes; *f* is the number of rotations (which is 1167 s^{-1} in our experiments); *R* is the radius of the centrifuge (the distance of the bottom of the tube to the centre, in this case 8 cm); and ρ_g is the density of graphene.

The two solvent properties, and therefore the variables relevant in this solvent screening, are the solvent density ρ_s and dynamic viscosity μ. According to equation 5 the ratio of density to viscosity will therefore influence the settling velocity of particles in suspension. A small density/dynamic viscosity ratio is desirable in this instance (equivalent to

the inverse of kinematic viscosity). We have proposed that a low settling velocity caused by high kinematic viscosity contributes to a higher concentration of dispersed graphene after centrifugation because of the increased stability of the dispersion. Evidence that viscosity is also related to the quality of graphene has also been provided (refer to Raman spectroscopy experiments in the main article and the Experiment Results section of this Supporting Information).

An arbitrary upper limit to the density/viscosity ratio of 1.20 g mL^{-1} cP^{-1} was implemented so to contain the recognised solvents with known high performance (NMP, DMF, and 1,2-DCB) but exclude enough solvents to justify the exercise. This produced 127 candidates from 199 entries. This was calculated independently of whether the polarity and surface tension of each solvent candidate was deemed as suitable or not. Of the solvent candidates with an ideal density to viscosity ratio, many are plasticisers, diols, and other glycerol derivatives too polar to qualify as graphene processing solvents (at least using the conditions reported here). Most of the bio-based solvents pass this criterion of the assessment, with the exception of 2-methyltetrahydrofuran, acetone, ethyl acetate, methanol, and tetrahydrofuran, and 8 further solvents without viscosity data (Table S7).

Table S7. Viscosity characteristics of the bio-based solvents.

Solvent name	**Density (ρ) /g mL^{-1}**	**Viscosity (μ) /g s^{-1} m^{-1}**	**ρ/μ**	**Status**
1,2-Pentanediol				No data
1,2-Propanediol	1.04	56	0.019	Pass
1,3-Propanediol				No data
1,4-Butanediol	1.02	84.9	0.012	Pass
1-Butanol	0.81	2.5	0.32	Pass

2-Butanol	0.80	3.0	0.27	Pass
2-Methyltetrahydrofuran	0.85	0.46	1.9	Fail
2-Octanol	0.82	6.5	0.13	Pass
2-Propanol	0.79	2.0	0.39	Pass
Acetic acid	1.04	1.1	0.99	Pass
Acetone	0.79	0.32	2.5	Fail
Acetyltributyl citrate	1.05	42.7	0.025	Pass
Butyl lactate	0.98	3.8	0.26	Pass
Butyric acid	0.96	1.4	0.67	Pass
Cyrene	1.25	14.5	0.086	Pass
Diethoxymethane				No data

Table S7. Viscosity characteristics of the bio-based solvents. (continued).

Solvent name	**Density (ρ) /g·mL^{-1}**	**Viscosity (μ) /g·s^{-1}·m^{-1}**	**ρ/μ**	**Status**
Dimethyl ether				No data
Dimethyl isosorbide	1.15	5	0.23	Pass
Dimethyl sulphoxide	1.10	2.0	0.55	Pass
d-Limonene	0.84	0.92	0.91	Pass
Ethanol	0.79	1.1	0.74	Pass
Ethyl acetate	0.89	0.44	2.0	Fail
Ethyl lactate	1.03	2.7	0.38	Pass
Ethylene glycol	1.11	16.1	0.069	Pass
Eugenol	1.07	7.8	0.14	Pass
Furfural	1.15	1.6	0.73	Pass
Furfuryl alcohol	1.13	4.6	0.24	Pass
Glycerol	1.25	954	0.0013	Pass
Glycerol carbonate	1.4	85	0.017	Pass

Glycerol formal	1.22	14.2	0.086	Pass
Isoamyl alcohol	0.81	4.2	0.19	Pass
Isobutanol	0.80	4.7	0.17	Pass
Isoeugenol	1.08	7.5	0.15	Pass
Lactic acid				No data
Lauric acid	0.87	7.3	0.12	Pass
Levulinic acid				No data
Methanol	0.79	0.54	1.5	Fail
Methyl lactate	1.09	2.9	0.38	Pass
Methyl oleate	0.87	4.9	0.18	Pass

Table S7. Viscosity characteristics of the bio-based solvents (continued).

Solvent name	**Density (ρ) /g·mL^{-1}**	**Viscosity (μ) /g·s^{-1}·m^{-1}**	**ρ/μ**	**Status**
Oleic acid	0.89	25.6	0.035	Pass
p-Cymene				No data
Solketal	1.07	11	0.097	Pass
t-Butyl ethyl ether				No data
Tetrahydrofuran	0.89	0.53	1.7	Fail
Tetrahydrofurfuryl alcohol	1.05	6.2	0.17	Pass
Triacetin	1.16	17.4	0.066	Pass
Triethyl citrate	1.14	35.2	0.032	Pass
α-Pinene	0.86	1.3	0.67	Pass
α-Terpineol	0.94	36.5	0.026	Pass
β-Pinene	0.86	1.5	0.57	Pass
γ-Valerolactone	1.05	2.2	0.48	Pass

Environmental health and safety. At this juncture it is prudent to review the current status of the solvent candidates. In total 22 solvents have the required polarity, viscosity, and

surface tension characteristics, including the benchmark solvents NMP, DMF, and 1,2-dichlorobenzene (Table S8). Environmental, health and safety (EHS) criteria were applied to the remaining 22 solvents. Five bio-based solvents are contained within this set. Levulinic acid did not have sufficient data to complete the viscosity assessment, but has recently been reported elsewhere as a viable graphene processing solvent.[34]

Table S8. Summary of solvent selection candidates.

Solvent	**Polarity**				**Surface tension /mN.m^{-1}**	**Viscosity /g·s^{-1}·m^{-1}**
	δ_D	δ_P	δ_H	Radius		
1,1,2,2-Tetrachloroethane	18.8	5.1	5.3	5.1	34.7	1.8
1,2,3-Trichloropropane	17.8	12.3	3.4	5.3	37.7	2.5
1,2-Dichlorobenzene	19.2	6.3	3.3	5.8	36.6	1.3
Acetophenone	18.8	9.0	4.0	4.0	39.8	1.7
Aniline	20.1	5.8	11.2	6.5	41.1	4.4
Benzaldehyde	19.4	7.4	5.3	4.2	38	1.3
Benzonitrile	18.8	12	3.3	5.4	38.8	1.3
Butyl lactate	15.8	6.5	10.2	5.8	35	3.8
Cyclohexanone	17.8	8.4	5.1	2.8	35.1	2.2
Cyclopentanone	17.9	11.9	5.2	3.6	33.2	1.29
Cyrene	18.8	10.6	6.9	2.2	33.6	14.5
Diethyl phthalate	17.6	9.6	4.5	3.3	37.5	12.9
Diethylene glycol monobutyl ether	16.0	7.0	10.6	5.5	32.8	4.9
Furfural	18.6	14.9	5.1	6.3	43.5	1.6
Morpholine	18.0	4.9	11.0	5.5	37.5	2.2
DMAc	16.8	11.5	9.4	3.7	32.4	0.9
DMF	17.4	13.7	11.3	5.8	35	0.8
Nitrobenzene	20.0	10.6	3.1	6.2	43.4	1.8

NMP	18.0	12.3	7.2	3.0	40.7	1.7
Pyridine	19.0	8.8	5.9	2.7	36.6	0.9
Tetrahydrofurfuryl alcohol	17.8	8.2	12.9	5.3	37	6.2
Triacetin	16.5	4.5	9.1	5.8	35.5	17.4

As a first pass greenness assessment, the safety datasheet (obtained from Sigma-Aldrich) of each of the 22 shortlisted solvents was used to immediately rule out candidates based on their toxicity profile (Table S9). Any solvent that causes cancer in humans, has been found to be mutagenic, or is reprotoxic was rejected in line with REACH CMR requirements (Table S3). Entries in orange in Table S9 indicate likely chronic toxicity in humans based on animal studies. Solvents that are severely acutely toxic (*e.g.* represented by any of the hazard statements H300, H301, H310, H331, H330, H331 as defined in the CLP directive) were also removed from the final candidate list, leaving only eight solvents remaining. No solvent candidates of the 22 on the shortlist were classifiable as PBT, although the aquatic toxicity of several candidates is high (see supplementary spreadsheet file).

Table S9. Solvent toxicology data screening.

Solvent	Carcino-genicity	Muta-genicity	Reproduc-tive toxicity	Acute toxicity
1,1,2,2-Tetrachloroethane				H310 & H330
1,2,3-Trichloropropane	Category 1B (H350)	Category 2 (H341)	Category 1B (H360)	H301 & H311 & H331
1,2-Dichlorobenzene	Pass			
Acetophenone		Positive animal tests		
Aniline	Category 2 (H351)	Category 2 (H341)		H301 & H311 & H331
Benzaldehyde		Positive animal tests		
Benzonitrile	Pass			
Butyl lactate	Pass			
Cyclohexanone	Pass			
Cyclopentanone	Pass			
Cyrene	Pass			
Diethyl phthalate			Positive animal tests	

Table S9. Solvent toxicology data screening. (continued).

Solvent	Carcino-genicity	Muta-genicity	Reproduc-tive toxicity	Acute toxicity
Diethylene glycol monobutyl ether	REACH restriction already in place: "*Shall not be placed on the market for supply to the general public, as a constituent of spray paints or spray cleaners in aerosol dispensers in concentrations equal to or greater than 3 % by weight*" (EU regulation (EC) No 1907/2006).			
Furfural	Category 2 (H351)	Positive animal tests		H301 & H331
Morpholine		Positive animal tests		
N,*N*-Dimethylacetamide			Category 2 (H360D)	
DMF			Category 2 (H360D)	
Nitrobenzene	Category 1B (H351)		Category 1B (H360F)	H301 & H311 & H331
NMP			Category 2 (H360)	
Pyridine	Pass			
Tetrahydrofurfuryl alcohol			Category 1B (H360Df)	
Triacetin	Pass			

Greenness assessment. The final phase of the solvent selection process relates to the greenness of each remaining solvent. The greenness assessment was only applied to the eight solvent candidates fulfilling the earlier performance requirements and EHS requirements to reduce the data gathering exercise. Cyrene is the only wholly bio-based solvent remaining. Butyl lactate is partially bio-based at present, as is triacetin. The technology exists to produce

wholly bio-based butyl lactate and triacetin, but the price and availability of bio-1-butanol and bio-based acetic acid means for the time being their petrochemical equivalents are used to produce the downstream solvents. This was not seen as a concern in the long term, with the lower threshold for bio-based solvents set at 25% bio-based carbon content (Table S4). For the 5 other solvents (1,2-dichlorobenzene, benzonitrile, cyclohexanone, cyclopentanone, and pyridine) the lack of a commercially proven renewable feedstock for manufacture is disadvantageous.

Greenness criteria were selected in an attempted to cover the different aspects of the solvent life cycle while also being validated by regulations. This exercise is not intended to rule out any of the final eight solvent candidates, instead its purpose is to create a hierarchy within these remaining solvents.

Seven physical property and toxicology data sets were obtained and related to consequential environmental, health and safety effects. The criteria were vapour pressure (low values are ideal to reduce VOC losses into atmosphere), autoignition temperature and flash point (for safety considerations), and rat oral LD_{50} (a health measure). In terms of environmental issues, lipophilicity (low logP values suggest a low potential for bioaccumulation) and aquatic toxicity were also considered in addition to biodegradability. Indicators for these criteria were presented earlier (Table S4). The greenness of the final eight solvent candidates can be compared to identify the most favourable options. A detailed examination is featured in the accompanying spreadsheet. For here it suffices to say that of the eight solvents, only triacetin is free of any breaches of legislated threshold values (Table S10). Butyl lactate and Cyrene are both VOCs. In addition to being VOCs, the five petrochemical solvents are all *harmful if swallowed* (whereas the bio-based solvents are not). Furthermore, 1,2-dichlorobenzene is hazardous to the aquatic environment, and cyclohexanone, cyclopentanone, and pyridine are all regarded as *flammable liquids* because

of their low flash points. For these reasons butyl lactate, Cyrene, and triacetin were employed as solvents in experimental graphene processing (Figure S12). The results are reported in the main article.

Table S10. Solvent greenness issues.

Solvent	Breaches of regulatory limits relating to solvent greenness
1,2-Dichlorobenzene	CLP 'acute toxicity' threshold (harmful if swallowed); Industrial emissions VOC definition; CLP 'harmful to the aquatic environment'.
Benzonitrile	CLP 'acute toxicity' threshold (harmful if swallowed); Industrial emissions VOC definition.
Butyl lactate	Industrial emissions VOC definition.
Cyclohexanone	CLP 'acute toxicity' threshold (harmful if swallowed); CLP 'flammable liquids' threshold; Industrial emissions VOC definition.
Cyclopentanone	CLP 'acute toxicity' threshold (harmful if swallowed); CLP 'flammable liquids' threshold; Industrial emissions VOC definition.
Cyrene	Industrial emissions VOC definition.
Pyridine	CLP 'acute toxicity' threshold (harmful if swallowed); CLP 'flammable liquids' threshold; Industrial emissions VOC definition.
Triacetin	None.

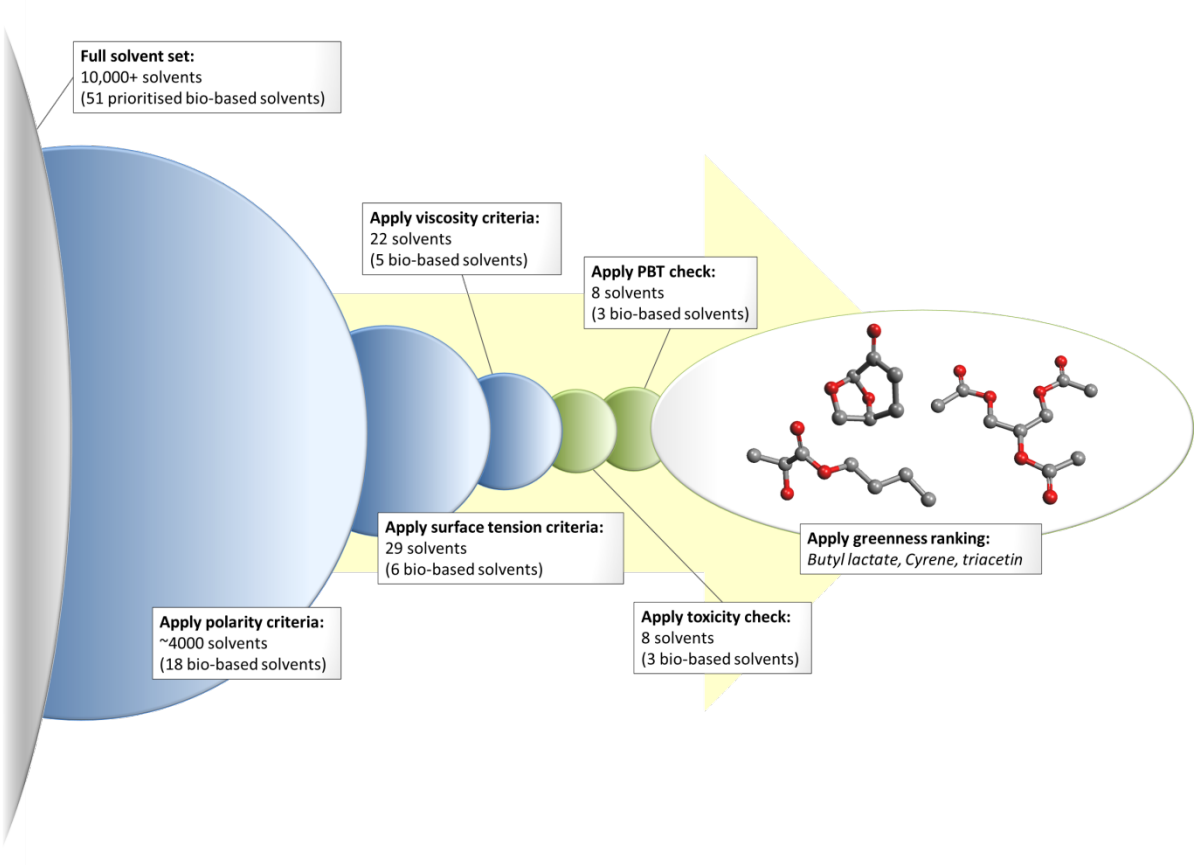

Figure S12. A schematic of the solvent selection process, refining a large dataset to three bio-based solvent candidates.

It should also be recognised that four of the solvents: benzonitrile, cyclohexanone, cyclopentanone, and pyridine, have been tested previously as graphene dispersion solvents,[26] and additionally 1,2-dichlorobenzene is an established solvent of course.[35] The prior existence of experimental data is useful to validate the solvent selection process, and can even be used to improve the protocol in subsequent reiterations. Of these solvents, cyclohexanone and cyclopentanone had previously been put forward as greener and more efficient graphene processing solvents.[29] Similarly benzonitrile also offered greater concentrations of graphene than NMP. In the same polarity relationship study pyridine was reported as a poor solvent,[26] which is unexpected from the conclusion of the solvent selection process in this work. One explanation could be the relatively low viscosity of pyridine for a graphene solvent, which is close to the cut-off threshold that was established in the solvent

selection process. Also note however that other reports show the successful use of pyridine as a graphene processing solvent,[36] and so the distinction between good and poor graphene processing solvents remains slightly elusive. That is why a multi-criteria solvent selection protocol was designed, and a number of solvent candidates shortlisted rather than only one.

Overview of advantages of Cyrene compared to NMP. Table S11 provides the numerical data given in Figure 1 of the main article.

Table S11. Relevant properties of Cyrene and NMP.

	Solvent properties	NMP	Cyrene
Physical properties	Density (ρ), g cm^{-3}	1.03	1.24
	Viscosity (μ), cP	1.7	10.5
	Surface tension (γ), mN m^{-1}	40.7	33.6
	Surface energy (ε),* mN m^{-1}	70.5	63.4
	Dispersive Hansen parameter (δ_D),§ $MPa^{0.5}$	18.0	18.8
	Polar Hansen parameter (δ_P),§ $MPa^{0.5}$	12.3	10.6
	Hydrogen bonding Hansen parameter (δ_H),§ $MPa^{0.5}$	7.2	6.9
Environmental health and safety considerations	Vapor pressure, mmHg	0.34	0.21
	Flash point (closed cup), °C	92	108
	Bio-based content	0%	100%
	logP	-0.38	-1.52

*Calculated according to the equation: $\gamma = \varepsilon - TS$, where the surface entropy, S takes the same value for both solvents,[3] of S ~ 0.1 mJ m^{-2} K^{-1}

§Calculated with HSPiP software.

Relevant information on other solvent selection guides.

There are other ways to compare Cyrene to NMP (and the other dipolar aprotic solvents) aside from the green-physicochemical assessment established in this work. These are worth considering to ensure the results presented here are not anomalous. Solvent selection guides can rate solvents according to performance or greenness.[37] Cyrene, as a relatively new solvent, only features in two solvent selection guides. These are the GSK tool (2016 version),[38] and the CHEM21 non-classical solvent tool.[39] Abbreviated versions of both, only considering the dipolar aprotic solvents, are provided (Table S12 and Table S13). Note the colour coding and scoring systems work on different principles, but green indicates a desirable score, and red an undesirable one.

Table S12. An excerpt of the GSK solvent selection guide (dipolar aprotic solvents).

Name	a	b	c	d	e	f	g	h	i	j	k	l
Cyrene	203	4*	4*	5	10	9*	6*	4*	8*	10*	10*	n/a
NMP	202	3	4	3	10	10	6	1	9	9	9	2
DMF	153	3	6	3	8	10	4	1	6	9	9	7
DMAc	165	3	6	3	9	10	6	1	7	9	9	2
DMSO	189	3	4	4	9	8	6	7	9	9	5	6

Key: a, boiling point /°C; b, incineration; c, recycling; d, bio-treatment; e, VOC emissions; f, aquatic impact; g, air impact; h, health hazard; i, exposure potential; j, flammability and explosion; k, reactivity and stability; l, life cycle analysis. High scores are considered desirable.
*Data gaps add uncertainty to the rank provided. There are nine data gaps in total for Cyrene across 8 categories.

Table S13. An excerpt of the CHEM21 solvent selection guide (dipolar aprotic solvents).

Name	S	H	E
Cyrene	1	2	7
NMP	1	9	7
DMF	3	9	5
DMAc	1	9	5
DMSO	1	1	5

Key: S, safety score; H, health score; E, environmental score. Low scores are considered desirable.

In the GSK tool Cyrene is shown to have notable advantages over the nitrogen containing dipolar aprotic solvents, in particular with respect to the health hazard score. As the only exclusively CHO molecule, the end-of-life categories all have satisfactory scores,

helped because no nitrogen or sulphur containing by-products form during incineration or biological waste treatments. As a word of caution, the complete properties of Cyrene needed to fulfil the GSK assessment are yet to all be determined. This may cause some of the scores to increase or decrease in the future as more data becomes available. Similarly, note that a score based on life cycle assessment is not possible for Cyrene yet.

The CHEM21 guide for use in the pharmaceutical industry appears less comprehensive by comparison, only having three categories. However there is a benefit to summarising the relevant data so succinctly for easier interpretation. What this does mean is that many considerations are behind each score and so the reason for the outcome is not immediately clear. The undesirable environment (E) score of Cyrene is actually due to its high boiling point, included in the assessment to recognise that energy intensive distillation is required in pharmaceutical product synthesis to separate and recycle solvents. Otherwise Cyrene is recognised as a green solvent.

It is important to remember that it is not only greenness that dictates solvent substitution, technical performance is also vital but it is very much specific to each different application. A solvent selection guide cannot tell you whether a solvent will be suitable for a process or formulation, or why that is so. This is why we did not rely on solvent selection guides to identify solvents for graphene production by liquid exfoliation. Furthermore, solvent selection guides are usually restricted to the set of solvents provided, although in this respect the CHEM21 assessment is easily transferable to new solvents. In this work we were able to screen a much larger number of solvents that would be feasible to display in terms of a solvent selection guide.

References

1. Court, G. R.; Lawrence, C. H.; Raverty, W. D; Duncan, A. J. Method for converting lignocellulosic materials into useful chemicals. World patent **2011**, WO 2011000030 A1.

2. Sherwood, J.; De bruyn, M.; Constantinou, A.; Moity, L.; McElroy,C. R.; Farmer, T. J.; Duncan, T.; Raverty, W.; Hunt, A. J.; Clark, J. H. Dihydrolevoglucosenone (Cyrene) as a bio-based alternative for dipolar aprotic solvents. *Chem. Commun.* **2014**, *50*, 9650-9652.

3. Hernandez,Y.; Nicolosi, V.; Lotya, M.; Blighe, F. M.; Sun, Z.; De, S.; McGovern, I. T.; Holland, B.; Byrne, M.; Gun'Ko, Y. K.; Boland, J. J.; Niraj, P.; Duesberg, G.; Krishnamurthy, S.; Goodhue, R.; Hutchison, J.; Scardaci, V.; Ferrari, A. C.; Coleman, J. N. High-yield production of graphene by liquid-phase exfoliation of graphite. *Nat. Nano.* **2008**, *3*, 563-568.

4. Graphenea. Graphenea Monolayer Graphene film - Product Datasheet. Available from: http://cdn.shopify.com/s/files/1/0191/2296/files/Graphenea_Monolayer_Film_Datasheet_2014-03-25.pdf?2923 (accessed 21/10/2015).

5. Wang, S.; Zhang, Y.; Abidi, N.; Cabrales, L. Wettability and surface free energy of graphene films. *Langmuir* **2009**, *25*, 11078-11081.

6. Coleman, J. N. Liquid exfoliation of defect-free graphene. *Acc. Chem. Res.* **2013**, *46*, 14-22.

7. Rafiee, J.; Mi, X.; Gullapalli, H.; Thomas, A. V.; Yavari, F.; Shi, Y.; Ajayan, P. M.; Koratkar, N. A. Wetting transparency of graphene. *Nat. Mater.* **2012**, *11*, 217-222.

8. Taherian, F.; Marcon, V.; van der Vegt, N. F. A.; Leroy, F. What is the contact angle of water on graphene? *Langmuir* **2013**, *29*, 1457-1465.

9. Salavagione, H. J.; Martínez, G.; Ellis, G. Graphene-Based Polymer Nanocomposites. In *Physics And Applications Of Graphene - Experiments*. Mikhailov, S., Eds.; InTech: Vienna, 2011; pp 169-192.

10. Li, Z.; Wang, Y.; Kozbial, A.; Shenoy, G.; Zhou, F.; McGinley, R.; Ireland, P.; Morganstein, B.; Kunkel, A.; Surwad, S. P.; Li, L.; Liu, H. Effect of airborne contaminants on the wettability of supported graphene and graphite. *Nat. Mater.* **2013**, *12*, 925-931.

11. Li, X.; Cai, W.; An, J.; Kim, S.; Nah, J.; Yang, D.; Piner, R.; Velamakanni, A.; Jung, I.; Tutuc, E.; Banerjee, S. K.; Colombo, L.; Ruoff, R. S. Large-area synthesis of high-quality and uniform graphene films on copper foils. *Science* **2009**, *324*, 1312-1314.

12. Reina, A.; Jia, X.; Ho, J.; Nezich, D.; Son, H.; Bulovic, V.; Dresselhaus, M. S.; Kong, J. Large area, few-layer graphene films on arbitrary substrates by chemical vapor deposition. *Nano. Lett.* **2009**, *9*, 30-35.

13. Malard, L. M.; Pimenta, M. A.; Dresselhaus, G.; Dresselhaus, M. S. Raman spectroscopy in graphene. *Phys. Rep.* **2009**, *473*, 51-87.

14. Pimenta, M. A.; Dresselhaus, G.; Dresselhaus, M. S.; Cançado, L. G.; Jorio, A.; Saito, R. Studying disorder in graphite-based systems by Raman spectroscopy. *Phys. Chem. Chem. Phys*. **2007**, *9*, 1276-1290.

15. Ferrari, A. C. Raman spectroscopy of graphene and graphite: disorder, electron–phonon coupling, doping and nonadiabatic effects. *Solid State Commun.* **2007**, *143*, 47-57.

16. Hao, Y.; Wang, Y.; Wang, L.; Ni, Z.; Wang, Z.; Wang, R.; Koo, C. K.; Shen, Z.; Thong, J. T. L. Probing layer number and stacking order of few-layer graphene by Raman spectroscopy. *Small* **2010**, *6*, 195-200.

17. Cançado, L. G.; Takai, K.; Enoki, T.; Endo, M.; Kim, Y. A.; Mizusaki, H.; Jorio, A.; Coelho, L. N.; Magalhães-Paniago, R.; Pimenta, M. A. General equation for the determination of the crystallite size La of nanographite by Raman spectroscopy. *Appl. Phys. Lett.* **2006**, *88*, 163106.

18. Cançado, L. G.; Jorio, A.; Martins Ferreira, E. H.; Stavale, F.; Achete, C. A.; Capaz, R. B.; Moutinho, M. V. O.; Lombardo, A.; Kulmala, T. S.; Ferrari, A. C. Quantifying defects in graphene via Raman spectroscopy at different excitation energies. *Nano Lett.* **2011**, *11*, 3190-3196.

19. Khan, U.; O'Neill, A.; Lotya, M.; De, S.; Coleman, J. N. High-concentration solvent exfoliation of graphene. *Small* **2010**, *6*, 864-871.

20. Sun, Z.; Vivekananthan, J.; Guschin, D. A.; Huang, X.; Kuznetsov, V.; Ebbinghaus, P.; Sarfraz, A.; Muhler, M.; Schuhmann, W. High concentration graphene dispersions with minimal stabilizer: a scaffold for enzyme immobilization for glucose oxidation. *Chem. Eur. J.* **2014**, *20*, 5752-5761.

21. Gani, R.; Jiménez-González, C.; Constable, D. J. C. Method for selection of solvents for promotion of organic reactions. *Computers & Chemical Engineering* **2005**, *29*, 1661-1676.

22. O'Neill, A.; Khan, U.; Nirmalraj, P. N.; Boland, J.; Coleman, J. N. Graphene dispersion and exfoliation in low boiling point solvents. *J. Phys. Chem. C* **2011**, *115*, 5422-5428.

23. Cheng, Q.; Debnath, S.; Gregan, E.; Byrne, H. J. Ultrasound-assisted SWNTs dispersion: effects of sonication parameters and solvent properties. *J. Phys. Chem. C* **2010**, *114*, 8821-8827.

24. Yousefinejad, S.; Honarasa, F.; Abbasitabar, F.; Arianezhad, Z. New LSER model based on solvent empirical parameters for the prediction and description of the solubility of buckminsterfullerene in various solvents. *J. Solution Chem.* **2013**, *42*, 1620-1632.

25. Kim, J. H.; Lee, J. H. Preparation of graphite nanosheets by combining microwave irradiation and liquid-phase exfoliation. *J. Ceram. Process. Res.* **2014**, *15*, 341-346.

26. Hernandez, Y.; Lotya, M.; Rickard, D.; Bergin, S. D.; Coleman, J. N. Measurement of multicomponent solubility parameters for graphene facilitates solvent discovery. *Langmuir* **2010**, *26*, 3208-3213.

27. Yi, M.; Shen, Z. G.; Zhang, X. J.; Ma, S. L. Achieving concentrated graphene dispersions in water/acetone mixtures by the strategy of tailoring hansen solubility parameters. *J. Phys. D: Appl. Phys.* **2013**, *46*, 025301.

28. CEN/TS 16766:2015. *Bio-based solvents - Requirements and test methods*. CEN/TC 411 Bio-based products: European Committe for Standardization (2015).

29. Hansen, C. M. In *Hansen Solubility Parameters: A User's Handbook*; CRC press: Boca Raton, 2007.

30. Bergin, S. D.; Sun, Z.; Rickard, D.; Streich, P. V.; Hamilton, J. P.; Coleman, J. N. Multicomponent solubility parameters for single-walled carbon nanotube−solvent mixtures. *ACS Nano* **2009**, *3*, 2340-2350.

31. Shin, Y. J.; Wang, Y.; Huang, H.; Kalon, G.; Wee, A. T. S.; Shen, Z.; Bhatia, C. S.; Yang, H. Surface-energy engineering of graphene. *Langmuir* **2010**, *26*, 3798-3802.

32. Lim, H. J.; Lee, K.; Cho, Y. S.; Kim, Y. S.; Kim, T.; Park, C. R. Experimental consideration of the hansen solubility parameters of as-produced multi-walled carbon nanotubes by inverse gas chromatography. *Phys. Chem. Chem. Phys.* **2014**, *16*, 17466-17472.

33. Xiong, B.; Cheng, J.; Qiao, Y.; Zhou, R.; He, Y.; Yeung, E. S. Separation of nanorods by density gradient centrifugation. *J. Chromatogr. A* **2011**, *1218*, 3823-3829.

34. Sharma, M.; Mondal, D.; Singh, N.; Prasad, K. Biomass derived solvents for the scalable production of single layered graphene from graphite. *Chem. Comm.* **2016**. DOI: 10.1039/C6CC00256K.

35. Hamilton, C. E.; Lomeda, J. R.; Sun, Z.; Tour, J. M.; Barron, A. R. High-yield organic dispersions of unfunctionalized graphene. *Nano Lett.* **2009**, *9*, 3460-3462.

36. Park, K. H.; Kim, B. H.; Song, S. H.; Kwon, J.; Kong, B. S.; Kang, K.; Jeon, S. Exfoliation of non-oxidized graphene flakes for scalable conductive film. *Nano Lett.* **2012**, 12, 2871-2876.

37. F. P. Byrne, S. Jin, G. Paggiola, T. H. M. Petchey, J. H. Clark, T. J. Farmer, A. J. Hunt, C. R. McElroy and J. Sherwood, Tools and techniques for solvent selection: green solvent selection guides. *Sustainable Chemical Processes*, **2016**, 4, 7.

38. C. M. Alder, J. D. Hayler, R. K. Henderson, A. M. Redman, L. Shukla, L. E. Shuster and H. F. Sneddon, Updating and further expanding GSK's solvent sustainability guide. *Green Chem.*, **2016**, 18, 3879-3890.

39. D. Prat, A. Wells, J. Hayler, H. Sneddon, C. R. McElroy, S. Abou-Shehada and P. J. Dunn, CHEM21 selection guide of classical- and less classical-solvents. *Green Chem.*, **2016**, 18, 288-296.